Metal Complexes Containing Allenylidene and Higher Cumulenylidene Ligands: A Theoretical Perspective

ARTICLE *in* ACCOUNTS OF CHEMICAL RESEARCH · SEPTEMBER 2011

Impact Factor: 22.32 · DOI: 10.1021/ar200009u · Source: PubMed

3 AUTHORS:

Cecilia Coletti
Università degli Studi G. d'Annunzio Chieti e …
56 PUBLICATIONS **714** CITATIONS
SEE PROFILE

Alessandro Marrone
Università degli Studi G. d'Annunzio Chieti e …
31 PUBLICATIONS **501** CITATIONS
SEE PROFILE

Nazzareno Re
Università degli Studi G. d'Annunzio Chieti e …
196 PUBLICATIONS **4,920** CITATIONS
SEE PROFILE

Metal Fragment Modulation of Metallacumulene Complexes: A Density Functional Study

Alessandro Marrone, Cecilia Coletti, and Nazzareno Re*

Dipartimento Scienze del Farmaco, Università G. D'Annunzio, I-66100 Chieti, Italy

Received May 28, 2004

Density functional calculations have been carried out on a series of metallacumulene complexes $L_mM(=C)_nH_2$ with several ML_m metal fragments to study the electronic structure, the bonding, and the reactivity of these complexes and how they are affected by the metal termini. The considered metal fragments include $[(Cp)_2(PH_3)Ti]$, $[Cp(PH_3)_2Mo]^+$, $[(CO)_5Cr]$, $[(CO)_5Mo]$, $[(CO)_5W]$, $[Cp(dppe)Fe]^+$, [*trans*-$Cl(dppe)_2Ru]^+$, $[Cp(PMe_3)_2Ru]^+$, $[BzCl(PH_3)Ru]^+$, [*trans*-$Cl(PH_3)_2Rh$], and [*trans*-$Cl(PH_3)_2Ir$], which are quite common in the chemistry of metal vinylidene, allenylidene, and higher cumulenes and range from a d^2 to a d^8 configuration and from electron-poor to electron-rich character. The optimized geometries calculated for the considered complexes have been found to be in good agreement with the available X-ray data and show that the peculiar carbon−carbon bond alternation superimposed to an average cumulenic structure, which is typical of these systems, is slightly perturbed by the nature of the metal fragment with the exception of the d^4 $[Cp(PH_3)_2Mo]^+$. Bonding energies have been calculated for all considered systems, and their dependence on the nature of the metal termini has been discussed. In particular an increase of the electron richness within d^6 metal fragments causes a slight decrease of metal−cumulene bond energy. On the other hand, bond energies for d^8 and, to a lesser extent, d^4−d^2 complexes are larger than those for the d^6 analogues. The charge distribution and the localization of the molecular orbitals have been employed to explain the known reactivity patterns of this class of complexes and to forecast their variation with the nature of the metal fragment for both even and odd chains.

Introduction

Metallacumulene complexes of the type $L_mM(=C)_nR_2$ are made of organic cumulenes $R_2C=(=C)_nR_2$ where a terminal carbon, $R_2C=$, is replaced by a double-bonded transition metal fragment L_nM. These complexes have recently received much attention since they can be potential precursors of molecular wires of interest in the field of novel optoelectronic materials and can also provide multifaceted reactive sites of interest in organic synthesis.[1−11] While several lower homologues with two (vinylidene complexes) and three (allenylidene complexes) carbon atoms are well known,[1,12−16] only a few examples have been reported with four or more carbon atoms.[4−9] Butatrienylidene metal complexes have been proposed as plausible intermediates,[8c] and only two have been recently isolated and structurally characterized by X-ray methods.[8a,b,d] Very few pentatetraenylidene metal complexes have been synthesized and fully characterized in the last years.[4−7,9] A heptahexaenylidene complex of chromium pentacarbonyl has been suggested as a plausible intermediate in the synthesis of some functionalized allenylidenes. Complexes with

* Corresponding author. Fax: +39 0871 3555267. E-mail: nre@unich.it.

(1) Bruce, M. I. *Chem. Rev.* **1998**, *98*, 2797.
(2) (a) Bruce, M. I. *Coord. Chem. Rev.* **1997**, *166*, 91. (b) Touchard, D.; Dixneuf, P. H. *Coord. Chem. Rev.* **1998**, *178*, 409.
(3) Cadierno, V.; Gamasa, M. P.; Gimeno, J. *Eur. J. Inorg. Chem.* **2001**, 571.
(4) Szafert, S.; Haquette, P.; Fallon, S. B.; Gladysz, J. A. *J. Organomet. Chem.* **2000**, *604*, 52.
(5) (a) Touchard, D.; Haquette, P.; Daridor, A.; Toupet, L.; Dixneuf, P. H *J. Am. Chem. Soc.* **1994**, *116*, 11157. (b) Peron, D.; Romero, A.; Dixneuf, P. H. *Gazz. Chim. Ital.* **1994**, *124*, 497. (c) Peron, D.; Romero, A.; Dixneuf, P. H. *Organometallics* **1995**, *14*, 3319.
(6) (a) Lass, R. W.; Steinert, P.; Wolf, J.; Werner, H. *Chem. Eur. J.* **1996**, *2*, 19. (b) Kovacik, I.; Laubender, M.; Werner, H. *Organometallics* **1997**, *16*, 5607.
(7) Roth, G.; Fischer, H. *Organometallics* **1996**, *15*, 1139.
(8) (a) Ilg, K.; Werner, H. *Angew. Chem., Int. Ed.* **2000**, *39*, 1632. (b) Ilg, K.; Werner, H. *Chem. Eur. J.* **2002**, *8*, 2812. (c) Bruce, M. I.; Hinterding, P.; Low, P. J.; Skelton, B. W.; White, A. W. *J. Chem. Soc., Chem. Commun.* **1996**, 1009. Lomprey, J. R.; Selegue, J. P. *Organometallics* **1993**, *12*, 616. Bruce, M. I.; Hinterding, P.; Tiekink, E. R. T.; Skelton, B. W.; White, A. H. *J. Organomet. Chem.* **1993**, *450*, 209. Bruce, M. I.; Hinterding, P.; Low, P. J.; Skelton, B. W.; White, A. H. *J. Chem. Soc., Dalton Trans.* **1998**, 467. Bruce, M. I.; Hinterding, P.; Ke, M.; Low, P. J.; Skelton, B. W.; White, A. H. *Chem. Commun.* **1997**, 715. (d) Venkatesan, K.; Fernàndez, F. J.; Blacque, O.; Fox, T.; Alfonso, M.; Schmalle, H. W.; Berke, H. *Chem. Commun.* **2003**, 2006.
(9) (a) Roth, G.; Fischer, H. *Organometallics* **1996**, *15*, 5766. (b) Roth, G.; Fischer, H.; Meyer-Friedrichsen, T.; Heck, J.; Houbrechts, S.; Persoons, A. *Organometallics* **1998**, *17*, 1511.
(10) Kovacik, I.; Gevert, O.; Werner, H.; Schmittel, M.; Söllner, R. *Inorg. Chim. Acta* **1998**, *275*−*276*, 435.
(11) Winter, R. F.; Klinkhammer, K.-W.; Záliׯf0. *Organometallics* **2001**, *20*, 1317.
(12) Bruce, M. I.; Swincer, A. G. *Adv. Organomet. Chem.* **1983**, *22*, 59. Bruce, M. I. *Chem. Rev.* **1991**, *91*, 197, and references therein.
(13) Fischer E. O.; Kalder H. J.; Frank, A.; Köhler, F. H.; Huttner, G. *Angew. Chem., Int. Ed. Engl.* **1976**, *15*, 623. Berke, H. *Angew. Chem., Int. Ed. Engl.* **1976**, *15*, 624. Fischer, H.; Reindl, D.; Roth, G. *Z. Naturforsch.* **1994**, *49b*, 1207.
(14) Binger, P.; Müller, P.; Wenz, R.; Mynott, R. *Angew. Chem., Int. Ed. Engl.* **1990**, *29*, 1037.
(15) (a) Selegue, J. P. *Organometallics* **1982**, *1*, 217. (b) Nickias, P. N.; Selegue, J. P.; Young, B. A. *Organometallics* **1988**, *7*, 2248
(16) Antonova, A. B.; Ioganson, A. A. *Russ. Chem. Rev. (Engl. Transl.)* **1989**, *58*, 693. Doherty, S.; Corrigan, J. F.; Carty, A. J.; Sappa, E. *Adv. Organomet. Chem.* **1995**, *37*, 39.

10.1021/om049615l CCC: $27.50
Publication on Web 09/10/2004

Scheme 1

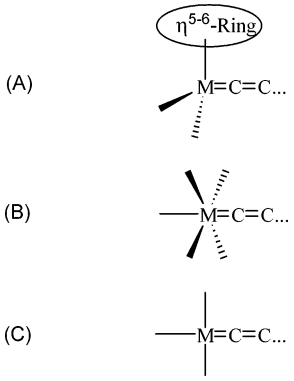

$n > 7$ have not been isolated or spectroscopically characterized so far.

Allenylidene and cumulenylidene complexes based on half-sandwich (A), octahedral (B), or square planar (C) metal fragments of group 6, 7, 8, and 9 with d^6 and d^8 electron counts are known,[1−12] while few vinylidenes of mainly half-sandwich d^4 metal fragment of group 6,[12,15b] and one allenylidene derivative of a d^2 metal fragment of group 4, $(Cp)_2(PMe_3)Ti(=C=C=CPh_2)$, have also been isolated (see Scheme 1).[14]

A few theoretical investigations have been performed on the simplest metallacumulene complexes[18−22] and, except for vinylidenes,[18] at mainly semiempirical level.[20−22] Only very recently have density functional calculations been performed on long chain metallacumulenes of the type $(CO)_5Cr(=C)_nR_2$,[23] $[Cl(PH_3)_4Ru(=C)_nH_2]^+$,[24] and $Cp(PH_3)_2Mn(=C)_4H_2$.[8d] In particular, two recent works of our group on $(CO)_5Cr(=C)_nR_2$ metallacumulene complexes of various lengths ($n = 2$, 9) and different substituents[23] have shown that (i) the geometries of even-chain cumulenes are consistent with a purely cumulenic structure, while the geometries of odd-chain cumulenes show a small but significant polyynyl carbon−carbon bond length alternation; (ii) the dissociation energies for the metal−cumulene bond are essentially independent of chain length, suggesting that there is no thermodynamic upper limit to the cumulene chain length; (iii) the regioselectivity of both electrophilic and nucleophilic attack is frontier orbital controlled with the LUMO mainly localized on the odd carbon atoms (C_1, C_3, C_5, ...) and the HOMO on the even carbon atoms (C_2, C_4, C_6, ...), determining, respectively, their electrophilic or nucleophilic character.

These conclusions have been confirmed by the DFT calculations of Saillard and co-workers on the $[Cl(PH_3)_4Ru(=C)_nH_2]^+$ ($n = 1-8$) series.[24]

In this paper we perform density functional theory (DFT) calculations on a series of metallacumulene complexes $L_nM(=C)_nH_2$ with several ML_m metal fragment types to study the electronic structure, the bonding, and the reactivity of these complexes and how they are affected by the nature of the metal termini. The considered metal fragments include $[(Cp)_2(PH_3)Ti]$, $[Cp(PH_3)_2Mo]$, $[(CO)_5Cr]$, $[(CO)_5Mo]$, $[(CO)_5W]$, $[Cp(dppe)Fe]^+$, $[trans\text{-}Cl(dppe)_2Ru]^+$, $[Cp(PMe_3)_2Ru]^+$, $[BzCl(PH_3)Ru]^+$, $[trans\text{-}Cl(PH_3)_2Rh]$, and $[trans\text{-}Cl(PH_3)_2Ir]$, which are quite common in the chemistry of metal vinylidene, allenylidene, and higher cumulenes and range from a d^2 to a d^8 configuration and from electron-poor to electron-rich character.

Since most characterized allenilydenes and metallacumulenes contain a d^6 metal center, many of the most common metal fragments with such an electron count have been considered. In particular, we considered $[(CO)_5Cr]$, $[(CO)_5Mo]$, and $[(CO)_5W]$, which are involved in some stable pentatetraenylidene and heptaexanylidene complexes recently synthesized,[7,9b] and some half-sandwich cationic ruthenium fragments, which are very common in the chemistry of cationic Ru(II) vinilydenes and allenylidenes and are expected to span a wide range of electron richness, as suggested by the oxidation potentials of the analogous chloride precursors: $(\eta^5\text{-}C_5Me_5)(PMe_2Ph)_2RuCl$, $E°_{1/2} = +0.15$ V;[17a] $trans\text{-}Cl_2(dppe)_2Ru$, $E°_{1/2} = +0.47$ V[2b]; $(\eta^6\text{-}C_6Me_6)(PMe_3)Cl_2Ru$, $E°_{1/2} = +0.77$ V[17b] versus standard calomel electrode (SCE). The considered d^8 rhodium and iridium fragments are involved in the newly developed chemistry of square-planar allenilydene complexes of Rh(I) and Ir(I), which show distinctly different properties.[6,8a] Although d^2 and d^4 allenilydene complexes are extremely rare and higher homologues unknown, the corresponding fragments have been considered since they are expected to show peculiar properties.

We have carried out geometry optimizations and studied the stability of these complexes and the nature of π conjugation along the metal and carbon atoms and their dependence on the nature of the metal fragment. We have also made use of the perturbational theory of reactivity, examining the charge distribution and the energies and localization of the frontier orbitals, to study the reactivity patterns of these complexes and their dependence on the nature of the metal termini.

Theoretical Calculations

The calculations reported in this paper are based on the ADF (Amsterdam Density Functional) program package.[25] The molecular orbitals were expanded in an uncontracted double-ζ Slater-type orbital (STO) basis set for all main group atoms. For all transition metal orbitals we used a double-ζ STO basis set for 3s and 3p and a triple-ζ STO basis set for 3d and 4s. As polarization functions, we used one 4p function for transi-

(17) (a) Le Lagadec, R.; Roman, E.; Toupet, L.; Miler, U.; Dixneuf, P. H. *Organometallics* **1994**, *13*, 5030. (b) Le Bozec, H.; Ouzzine, K.; Dixneuf, P. H. *Organometallics* **1991**, *10*, 2768.

(18) Stegmann, R.; Frenking, G. *Organometallics* **1998**, *17*, 2089. Wakatsuki, Y.; Koga, N.; Werner, H.; Morokuma, K. *J. Am. Chem. Soc.* **1997**, *119*, 360. De Angelis, F.; Sgamellotti, A.; Re, N. *Organometallics* **2002**, *21*, 2715.

(19) Ehlers, A. W.; Dapprich, S.; Vyboishchikov, S. F.; Frenking, G. *Organometallics* **1996**, *15*, 105.

(20) Schilling, B. E. R.; Hoffmann, R.; Litchenberger, D. L. *J. Am. Chem. Soc.* **1979**, *101*, 585. Schilling, B. E. R.; Hoffmann, R.; Faller, J. W. *J. Am. Chem. Soc.* **1979**, *101*, 592. Kostić, N. M.; Fenske, R. F. *Organometallics* **1982**, *1*, 974.

(21) Berke, H.; Huttner, G.; von Seyerl, J. *Z. Naturforsch., B: Anorg. Chem., Org. Chem.* **1981**, *36B*, 1277.

(22) Esteruelas, M. A.; Gómes, A. V.; López, A. M.; Modrego, J.; Oñate, E. *Organometallics* **1997**, *16*, 5826. Cadierno, V.; Gamasa, M. P.; Gimeno, J.; Gonzàles-Cueva, M.; Lastra, E.; Borge, J.; Garcìa-Granda, S.; Pérez-Carreño, E. *Organometallics* **1996**, *15*, 2137. Cadierno, V.; Gamasa, M. P.; Gimeno, J.; Lòpez-Gonzàles, M. C.; Borge, J.; Garcìa-Granda, S. *Organometallics* **1997**, *16*, 4453.

(23) (a) Re, N.; Sgamellotti, A.; Floriani, C. *Organometallics* **2000**, *19*, 1115. (b) Marrone A.; Re, N. *Organometallics* **2002**, *21*, 3562.

(24) Auger, N.; Touchard, D.; Rigaut, S.; Halet, J.-F.; Saillard, J.-Y. *Organometallics* **2003**, *22*, 1638.

(25) Baerends, E. J.; Ellis, D. E.; Ros, P. *Chem. Phys.* **1973**, *2*, 42. Boerrigter, P. M.; te Velde, G.; Baerends, E. J. *Int. J. Quantum Chem.* **1988**, *33*, 87.

tion metals, one 3d for C and O, and one 2p for H. The inner shell cores have been kept frozen.

The LDA exchange−correlation potential and energy were used, together with the Vosko−Wilk−Nusair parametrization[26] for homogeneous electron gas correlation, including Becke's nonlocal correction[27a] to the local exchange expression and Perdew's nonlocal correction[27b] to the local expression of correlation energy. Molecular structures of all considered complexes were optimized at this nonlocal (NL) level in the appropriate (C_1, C_s, or C_{2v}) symmetry.

Since the relativistic effects play an important role in describing the electronic structure and relative energetics of the species containing a heavy metal, such as tungsten and iridium, they were taken into account by the Pauli formalism, the Pauli Hamiltonian including first-order scalar relativistic corrections (Darwin and mass velocity) while neglecting spin−orbit corrections.[28]

Throughout the paper only butatrienylidenes and pentatetraenylidenes have been considered as representatives of even- and odd-chain cumulenes, respectively; it has indeed been shown that no significant effects are to be expected by either increasing or decreasing the length of the chains.[23]

For metal fragments with C_s symmetry there can be two different orientations of the cumulene C_nH_2 moiety, which may lie in the symmetry plane of the molecule or perpendicular to it. In these complexes we optimized both possible cumulene orientations and discussed only the most stable one.

Results and Discussion

d^6 Complexes: Electron-Richness Effects. All complexes have been fully optimized under C_{2v}, C_s, or C_1 symmetry and show $^1A_1$ ground states, with almost linear cumulene chains. The optimized bond lengths within the cumulene unit are reported in Figure 1. For those metal fragments with C_s symmetry the minimum energy orientation of the cumulene moiety corresponds to that expected on the basis of simple MO models:[20] the plane of the odd-chain C_5H_2 cumulene (i.e., the plane defined by the terminal HCH triangle) lies in the symmetry plane of the fragment, while the plane of the even-chain C_4H_2 cumulene lies perpendicular to it. This orientation is preferred since it allows a more efficient π back-donation from the highest occupied d_π metal orbital of a″ symmetry to the cumulene LUMO which lies in the plane in even chains and perpendicular to it in odd chains (see below).

The geometries of the even-chain C_4 complexes are consistent with a purely cumulenic structure, with C−C bond lengths ranging from 1.26 to 1.29 Å, except for the terminal C−C bond, which is markedly longer (1.31−1.34 Å), as expected for a sp^2 hybridation of the terminal carbon atom. On the other hand, as it was found in ref 23 for [(CO)$_5$Cr]-cumulenes, the geometries of odd-chain C_5 complexes show a polyynyl carbon−carbon bond length alternation superimposed to an average cumulenic structure with two distinct types of C−C bond lengths, falling in the ranges 1.26−1.28 and 1.30−1.31 Å, respectively. This is consistent with the contribution of stable zwitterionic polyynyl resonance structures for

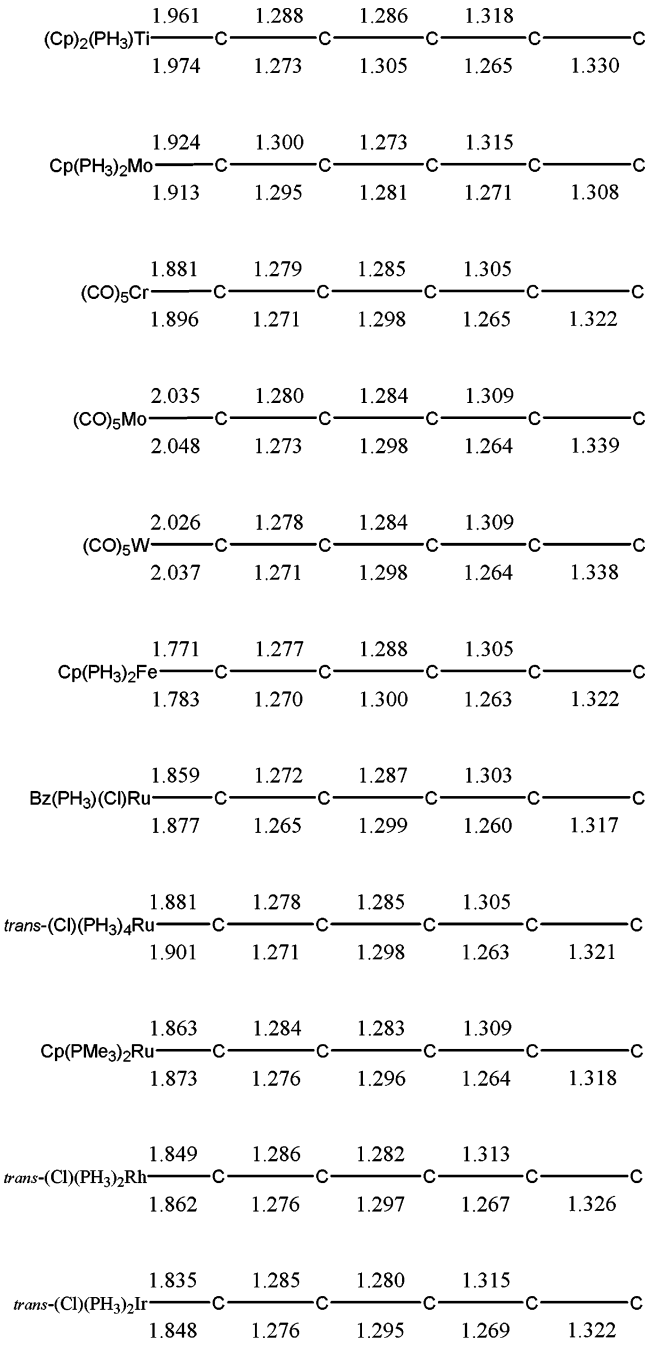

Figure 1. Optimized bond lengths (Å) for the cumulene unit in [L$_m$M(=C)$_n$H$_2$] complexes with $n = 4, 5$ ranging from d^2 to d^8 metal fragments.

Scheme 2

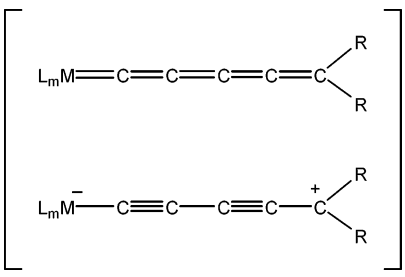

C_5 and, in general, for odd cumulene chains, as depicted in Scheme 2. The extent of this alternation is also slightly affected by the metal fragment character: it is

(26) Vosko, S. H.; Wilk, L.; Nusair, M. *Can. J. Phys.* **1980**, *58*, 1200.
(27) (a) Becke, A. D. *Phys. Rev. A* **1988**, *38*, 2398. (b) Perdew, J. P. *Phys. Rev. B* **1986**, *33*, 8822.
(28) Ziegler, T.; Tshinke, V.; Baerends, E. J.; Snijders, J. G.; Ravenek, W. *J. Phys. Chem.* **1989**, *93*, 3050. Boerrigter, P. M. Spectroscopy and Bonding of Heavy Element Compounds. Thesis, Vrije University, 1987. Li, J.; Schreckenbach, G.; Ziegler, T. *J. Am. Chem. Soc.* **1995**, *117*, 486, and references therein.

Table 1. Experimental M−C and C−C Distances (Å) for Some Butatrienylidene and Pentatetraenylidene Complexes

complex	M−C$_1$	C$_1$−C$_2$	C$_2$−C$_3$	C$_3$−C$_4$	C$_4$−C$_5$
trans-Cl(PPr$^i_2$)$_2$Ir(=C)$_4$Ph$_2$[8a]	1.816(6)	1.283(8)	1.275(8)	1.339(8)	
trans-Cl(PPr$^i_2$)$_2$Ir(=C)$_5$Ph$_2$[6a]	1.834(5)	1.261(6)	1.296(8)	1.259(6)	1.344(6)
(CO)$_5$Cr(=C)$_5$NEt$_2$CMe=C(NMe)$_2$[9b]	2.041(6)	1.219(8)	1.379(8)	1.209(9)	1.433(8)
(CO)$_5$W(=C)$_5$(NMe$_2$)$_2$[7]	2.144(6)	1.223(9)	1.361(9)	1.192(9)	1.399(9)
trans-[Cl(dppe)$_2$Ru(=C)$_5$Ph$_2$]$^+$ [5a]	1.891(9)	1.25(1)	1.30(1)	1.24(1)	1.36(1)

smaller for electron-rich metal fragments, such as [Cp(PMe$_3$)$_2$Ru]$^+$ complexes, while it becomes more pronounced for electron-poor metal fragments, such as [BzCl(PH$_3$)Ru]$^+$ complexes. This is a consequence of the destabilization of the zwitterionic resonance structures when a negative formal charge is located on an electron-rich fragment, thus leading to a decrease in the polyynyl character of the complex.

In both even- and odd-chain complexes the M−C distances (1.77 Å for M = Ru) are consistent with a double-bond character and are only weakly affected by the metal fragments; for instance going from the electron-poor fragment [BzCl(PH$_3$)Ru]$^+$ to the electron-rich [Cp(PMe$_3$)$_2$Ru]$^+$, the Ru−C distance varies within 1.859−1.891 Å (even-chain) or 1.873−1.901 Å (odd-chain). Moreover, because of the partial single character shown by the resonance structures in Scheme 2, in each complex the M−C distance for the C$_4$ chain is shorter than the corresponding one for the C$_5$ chain by ca. 0.01−0.02 Å.

In Table 1 we report the experimental X-ray data for some representative butatrienylidene and pentatetraenylidene complexes.[5a,6a,7,8a,9b] Although the bond alternation is slightly underestimated by ca. 0.02−0.04 Å, the overall agreement is rather good and, as discussed in previous papers,[23] the underestimation is most likely determined by the presence of the methyl, ethyl, phenyl, or alkenyl groups in the experimental complexes, which are expected to stabilize the polyynyl resonance structures, thus enhancing the bond alternation. The calculated electron-richness trend, i.e., the more electron rich the metal fragments, the less pronounced the alternation in the cumulene bond lengths, is confirmed by a recent experimental study of Fischer and co-workers on allenylidene complexes.[29] Indeed, in a series of *cis*-[(CO)$_4$(PR$_3$)Cr=C=C=C(R$_1$)R$_2$] complexes they observed that an increase of the electron-donor properties of PR$_3$ leads to a shift of the ν(CCC) band in the IR spectrum to lower energy, thus indicating a more allene-like structure. This effect was also confirmed by a low-field shift of the ^{13}C resonance of the metal-bound Cα atom and by a shift of the MLCT transition in the UV−vis spectrum toward longer wavelengths.

The electronic structures of the metallacumulenic complexes can be usefully discussed in terms of the orbital interactions between the metal L$_m$M and the cumulenic (=C)$_n$H$_2$ fragments. The frontier orbitals of the free cumulenes C$_n$H$_2$ are described in ref 23 and are made up by a set of n out-of-plane π orbitals (hereafter called $\pi_\perp$, all of b_1 symmetry) and a set of $n-1$ in-plane π orbitals (hereafter called $\pi_{||}$, all of b_2 symmetry), occupied by $2n-2$ electrons. The frontier orbitals for the octahedral [(CO)$_5$M] and [*trans*-Cl(dppe)$_2$Ru]$^+$ or pseudo-octahedral [Cp(dppe)Fe]$^+$ and [Cp(PMe$_3$)$_2$Ru]$^+$ fragments with one ligand removed are known[19,23,24] and show essentially the same pattern with a low-lying empty d orbital of σ symmetry with respect to the metal cumulene axis (d_{z^2}), two high lying almost degenerate filled orbitals of π symmetry (d_{xz} and d_{yz}), and a lower lying filled d orbital of δ symmetry (d_{xy}). An analogous pattern is also shown by the asymmetric [BzCl(PH$_3$)Ru]$^+$ fragment. These orbitals are affected by the electron richness of the metal center, and in particular, fragments with an increasing electron richness show a progressive raising of the energy of both HOMO and LUMO orbitals, as illustrated in Figure 2 for the Ru(II) series, i.e., [BzCl(PH$_3$)Ru]$^+$ → [*trans*-Cl(dppe)$_2$Ru]$^+$ → [Cp(PMe$_3$)$_2$Ru]$^+$.

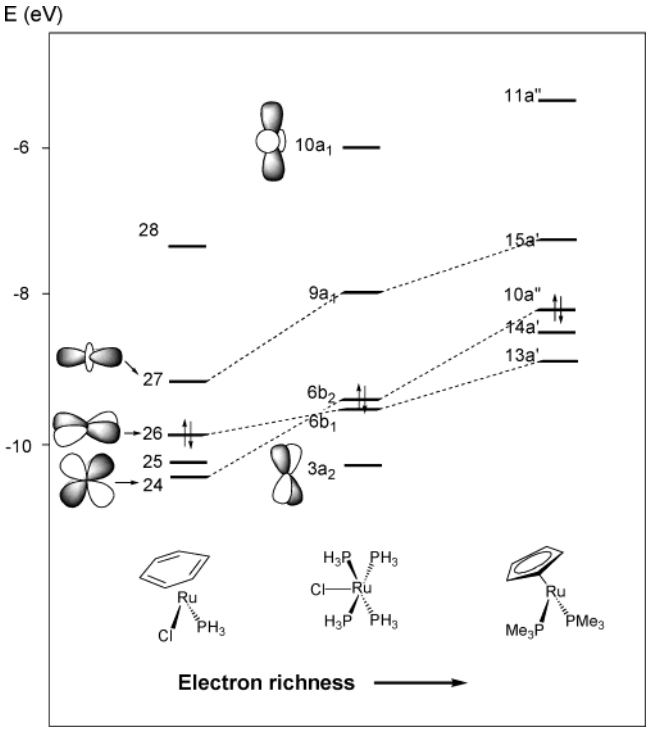

Figure 2. Frontier orbitals for Ru(II) metal fragments with increasing electron richness.

The main interaction between the L$_m$M and C$_n$H$_2$ fragments in all d^6 complexes (as well as in d^8 complexes described in the next section) can be basically summarized into three types: (i) a σ donation occurs from the cumulene lone pair to the empty dσ metal orbital; (ii) one filled dπ orbital back-donates into the empty cumulene LUMO; (iii) the other filled dπ orbital interacts with the filled cumulene HOMO and the empty LUMO+1; the former interaction is a destabilizing two-orbital four-electron interaction, while the latter is a minor stabilizing back-donation interaction. The pure back-donation occurs into a $\pi_{||}$ LUMO when n is even and into a $\pi_\perp$ when n is odd. As an example Figure 3 shows the orbital interaction diagram for [Cp(PMe$_3$)$_2$-

(29) Szesni, N.; Weibert, B.; Fischer, H. *Inorg. Chim. Acta* **2004**, *357*, 2939.

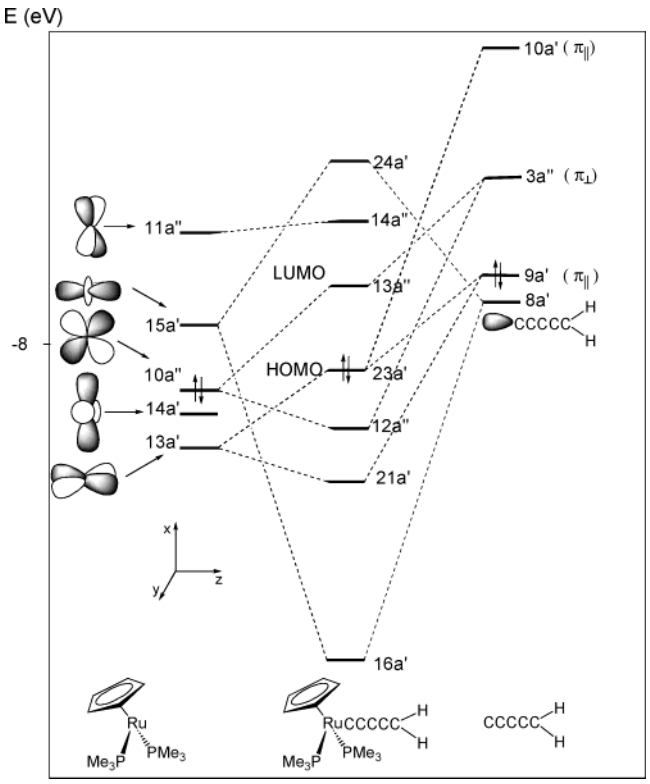

Figure 3. Orbital interaction diagram for the complex $[Cp(PMe_3)_2Ru(=C)_5H_2]^+$.

$Ru(=C)_5H_2]^+$. The diagram shares essentially the same features as that for $(CO)_5Cr(=C_5)H_2$ described in ref 23. However the analysis of the trend in the orbital interactions as the electron richness in d^6 fragments increases is particularly interesting: the metal dπ orbitals rise closer to the cumulene LUMO and π back-donation increases, while at the same time the metal dσ rises further from the cumulene lone pair and σ donation decreases. These trends are reflected in the bond dissociation energies reported in Table 2 and calculated according to the fragment-oriented approach of the DFT computational scheme implemented in the ADF program by the equation

$$D = E^* + E^R_{LnM} + E^R_{CnH2} \quad (1)$$

First we calculate the "snapping energies", $E^*(Cr{-}C_nX_2)$, i.e., the energies gained when snapping the metal−cumulene bond, obtained by building $(CO)_5Cr(=C)_nX_2)$ from the fragments with the conformation they assume in the equilibrium geometry of the overall complex. Then we compute the energies E^R_{LnM} and E^R_{CnH2} gained when the isolated fragments relax to their equilibrium geometries. Corrections for the zero-point vibrations or BSSE were not included since they are expected to be quite small.[23]

Table 2 shows that both snapping energies and bond dissociation energies do not follow any trend related to the different electron richness of the fragments in the Ru(II) series. This is obviously a consequence of the simultaneous decreasing of σ donation and increasing of π back-donation: the two effects tend to cancel out, so that the bonding energies of Table 2 do not show a monotonic variation with the electron richness.

Table 2. Calculated Bond Dissociation Energies for the $L_mM(=C)_nH_2$ Complexes (kJ mol^{-1})

complex	n	E^*	E^R_{MLm}	E^R_{CnH2}	D_e
$(Cp)_2(PH_3)Ti(=C)_nH_2$	4	406	53	1	352
	5	441	56	1	384
$[(Cp)(PH_3)_2Mo(=C)_nH_2]^+$	4	463	64	2	397
	5	500	67	2	431
$(CO)_5Cr(=C)_nH_2$	4	296	10	2	276
	5	294	10	2	282
$(CO)_5Mo(=C)_nH_2$	4	280	25	1	254
	5	291	27	2	262
$(CO)_5W(=C)_nH_2$	4	332	21	1	310
	5	341	21	2	318
$[(Cp)(PH_3)_2Fe(=C)_nH_2]^+$	4	389	15	1	373
	5	402	15	2	385
$[(Bz)Cl(PH_3)Ru(=C)_nH_2]^+$	4	412	96	1	315
	5	421	90	2	329
$[trans\text{-}Cl(PH_3)_2Ru(=C)_nH_2]^+$	4	371	8	1	362
	5	381	7	1	373
$[(Cp)(PH_3)_2Ru(=C)_nH_2]^+$	4	393	32	1	360
	5	404	29	2	373
$[trans\text{-}Cl(PH_3)_2Rh(=C)_nH_2]^+$	4	388	6	1	381
	5	397	6	1	390
$[trans\text{-}Cl(PH_3)_2Ir(=C)_nH_2]^+$	4	508	7	1	500
	5	516	6	1	509

The bonding in the considered metallacumulene fragments has been discussed by the Dewar−Chatt−Duncanson model in terms of a synergistic σ donation π back-donation.[30] The contribution from σ and π back-donation can be separately evaluated by decomposing the bond dissociation energy into a number of contributions,[31a] namely, the energy needed to convert the fragments from their equilibrium geometries to the geometries assumed in the optimized complex, E_{prep} (here given by the sum of the relaxation energies $E^R_{CnH2} + E^R_{MLn}$), the electrostatic interaction between the two fragments, E_{elstat}, the repulsive interaction between the fragments due to the antisymmetry requirement on the total wave function, $E_{Pauli,}$ and the stabilizing orbital interaction term, E_{orb}:

$$D(ML_n - C_nH_2) = -(E_{prep} + E_{elstat} + E_{Pauli} + E_{orb}) \quad (2)$$

The latter term, E_{orb}, which represents the attracting orbital interactions leading to the energy lowering upon coordination, can in turn be decomposed into contributions from the orbital interactions within the various irreducible representations Γ of the overall symmetry group of the system according to Ziegler.[31b] For complexes of C_{2v} symmetry, the ligand to metal donation takes place into the A_1 representation, while the metal to ligand back-donation takes place into the B_1 and B_2 representations. In particular for odd chains, E_{B1} is the energy contribution from the back-donation into the LUMO while E_{B2} is the contribution from the π interaction in the orthogonal plane (two-orbital four-electron repulsion plus back-donation into the LUMO+1) and is therefore expected to be smaller; on the other hand, for even chains the role of the two contributions is exactly exchanged. For complexes showing C_s symmetry, σ donation and the combined two-orbital four-electron repulsion plus back-donation into the LUMO+1 occur into the A′ representation while the π back-donation into

(30) Dewar, M. J. S. *Bull. Soc. Chim. Fr.* **1951**, *18*, C71. Chatt, J.; Duncanson, L. A. *J. Chem. Soc.* **1953**, 2939.

(31) (a) Ziegler, T.; Rauk, A. *Theor. Chim. Acta* **1977**, *46*, 1. (b) Ziegler, T. *NATO ASI* **1986**, *C176*, 189.

Table 3. Bond Dissociation Energy Decomposition for the $L_mM(=C)_nH_2$ Complexes (kJ mol^{-1})

					$E_{A'}$		$E_{A''}$	
complex	n	E_{Pauli}	E_{elstat}	E_{orb}	E_{A1}	E_{A2}	E_{B1}	E_{B2}
$(Cp)_2(PH_3)Ti(=C)_nH_2$	4	596	−441	−562	−518		−44	
	5	585	−441	−587	−547		−39	
$[(Cp)(PH_3)_2Mo(=C)_nH_2]^+$	4	841	−663	−641	−532		−109	
	5	885	−704	−681	−557		−124	
$(CO)_5Cr(=C)_nH_2$	4	626	−496	−415	−196	0	−75	−147
	5	608	−492	−410	−196	0	−148	−68
$(CO)_5Mo(=C)_nH_2$	4	599	−482	−398	−169	0	−75	−154
	5	604	−492	−403	−171	0	−162	−69
$(CO)_5W(=C)_nH_2$	4	695	−577	−451	−204	0	−82	−165
	5	680	−575	−446	−203	0	−169	−74
$[(Cp)(PH_3)_2Fe(=C)_nH_2]^+$	4	759	−638	−510	−318		−191	
	5	737	−638	−502	−310		−192	
$[(Bz)Cl(PH_3)Ru(=C)_nH_2]^+$	4	1138	−872	−679	−679			
	5	1056	−841	−638	−638			
$[trans\text{-}Cl(PH_3)_2Ru(=C)_nH_2]^+$	4	897	−739	−529	−253	0	−100	−176
	5	852	−723	−510	−248	0	−90	−173
$[(Cp)(PH_3)_2Ru(=C)_nH_2]^+$	4	989	−790	−558	−367		−191	
	5	963	−786	−557	−364		−193	
$[trans\text{-}Cl(PH_3)_2Rh(=C)_nH_2]^+$	4	910	−737	−565	−213	1	−100	−249
	5	877	−722	−551	−209	1	−89	−254
$[trans\text{-}Cl(PH_3)_2Ir(=C)_nH_2]^+$	4	1180	−954	−735	−319	0	−122	−295
	5	1146	−937	−725	−317	0	−109	−299

the LUMO occurs into the A″ representation. Such an analysis is obviously not possible for the $[BzCl(PH_3)RuC_nH_2]^+$ complexes of C_1 symmetry. The results of this decomposition are shown in Table 3. It is worth noting that for C_{2v} symmetry complexes, for which a full separation of the energy contributions due to σ donation and π back-donation is possible, the overall contribution to the orbital interaction term from π back-donation, $E_{B1} + E_{B2}$, is slightly higher than that from σ donation, E_{A1}, the same results already found for $(CO)_5Cr(=C)_nH_2$.[23] The effect of electron richness is more difficult to detect due to the different symmetries of the involved complexes. Such an effect is clear but weak in the $(CO)_5M(=C)_nH_2$ series (M = Cr, Mo, or W) of C_{2v} symmetry: there is a small increase of π back-donation ($E_{B1} + E_{B2}$) with the electron richness, by ca. 10−15 kJ mol^{-1}, but no definite trend for the values of E_{A1} corresponding to σ donation. For the Ru(II) series a comparison can be made only between the E_{B2} contribution for $[trans\text{-}Cl(dppe)_2Ru(=C)_nH_2]^+$ and the $E_{A''}$ contribution for $[Cp(PMe_3)_2Ru(=C)_nH_2]^+$, both corresponding to π back-donation into the LUMO. The contribution for the less electron-rich $[trans\text{-}Cl(dppe)_2Ru](=C)_nH_2]^+$, 173−176 kJ mol^{-1}, is smaller than that for the more electron-rich $[Cp(PMe_3)_2Ru(=C)_nH_2]^+$, 191−193 kJ mol^{-1}, thus confirming that π back-donation increases with electron richness. Assuming analogous increases, of ca. 20 kJ mol^{-1}, for the π back-donation into the LUMO+1 in $[Cp(PMe_3)_2Ru(=C)_nH_2]^+$ and subtracting it from the $E_{A'}$ contribution we can estimate the energetic contribution due to σ donation as 247 and 254 kJ mol^{-1}, which are very close to those of $[trans\text{-}Cl(dppe)_2Ru(=C)_nH_2]^+$, 253 and 248 kJ mol^{-1}, confirming again that the decrease of σ donation forecasted on the basis of orbital energy considerations (vide supra) is actually negligible.

The investigation of the reactivity and regioselectivity of the studied complexes toward both nucleophilic and electrophilic attacks has also been carried out. Although the reactivity of vinylidene and allenylidene metal complexes is well known, the available data on that of higher metallacumulenes are quite scarce. As far as complexes with d^6 metal fragments are concerned, there is evidence of ruthenium cationic butatrienylidenes undergoing only nucleophilic attack at C_3 and the few available data for the known pentatetraenylidene complexes give evidence for regioselective nucleophilic attack at C_1, C_3, or C_5 and electrophilic attack at C_2.[5−7,9,10]

In the present work we have analyzed the reactivity and regioselectivity for the d^6 complexes, with special emphasis on the effects of the increasing electron richness in the metal moiety, according to the approach developed by Fukui and generalized by Klopman, which distinguishes between charge-controlled and frontier-controlled reactions.[32,33] The results of a Mulliken population analysis calculating the gross atomic charges on the metal and the various carbon atoms of the cumulene ligand are reported in Table S1 and show no significant charge differences among the central carbon atoms of the cumulene chains, indicating that charge distribution is not important in determining the regioselectivity of either electrophilic or nucleophilic attack, as already observed for the $(CO)_5Cr(=C)_nH_2$ complexes. The analysis of the molecular orbital energies (Table 4a) shows that all the investigated cumulenes present relatively high lying HOMOs and low lying LUMOs, suggesting that the reactivity of these complexes toward both electrophilic and nucleophilic attack is again determined by frontier orbital factors. Moreover, since the HOMOs are quite isolated in energy from the other highest occupied MOs and the LUMOs are even better isolated from the other lowest unoccupied orbitals, these two orbitals play the main role in determining the regioselectivity of, respectively, the electrophilic and nucleophilic attack. However, as was underlined in the discussion of the orbital interaction diagram, the energy of the LUMOs of the complexes rises with the electron richness, thus leading to a reduced reactivity toward

(32) Fukui, K.; Yonezawa, T.; Nagata, C. *J. Chem. Phys.* **1957**, *27*, 1247. Fukui, K.; Yonezawa, T.; Nagata, C. *J. Chem. Phys.* **1959**, *31*, 550. Fukui, K. *Theory of Orientation and Stereoselection*; Springer: Berlin, 1975.

(33) Klopman, G.; Hudson, R. F. *Theor. Chim. Acta* **1967**, *8*, 1965. Klopman, G. *J. Am. Chem. Soc.* **1968**, *90*, 223. Klopman, G. In *Chemical Reactivity and Reaction Paths*; Klopman, G., Ed.; Wiley: New York, 1974; pp 59−67.

Table 4. Orbital Energies and Breakdowns of the Orbital Contributions from the Metal and Cumulene Carbon Atoms for the Frontier Orbitals of d^6 Complexes

complex	*n*	ϵ	orbital	M	C_1	C_2	C_3	C_4	C_5
$(CO)_5Cr(=C)_nH_2$	4	−6.083	HOMO	38.6	4.6	16.5	1.8	18.8	
		−4.645	LUMO	12.8	33.1	3.6	32.6		
	5	−6.006	HOMO	37.2	6.4	16.3	2.7	15.5	
		−5.188	LUMO	13.8	20.1	7.2	20.1	3.2	26.6
$(CO)_5Mo(=C)_nH_2$	4	−5.885	HOMO	36.5	4.2	15.9	0.0	18.1	
		−4.518	LUMO	9.1	32.7	1.1	31.2		
	5	−5.802	HOMO	34.3	6.1	16.4	1.6	15.5	
		−5.022	LUMO	11.3	19.7	4.4	19.2	1.7	26.4
$(CO)_5W(=C)_nH_2$	4	−5.911	HOMO	33.2	4.2	16.0	0.0	18.4	
		−4.561	LUMO	8.1	31.8	0.0	30.6		
	5	−5.841	HOMO	31.9	5.8	16.1	1.6	15.3	
		−5.076	LUMO	10.4	19.3	4.5	19.0	1.7	26.3
$[(Cp)(PH_3)_2Fe(=C)_nH_2]^+$	4	−8.971	HOMO	37.9	9.7	18.3	2.8	23.1	
		−7.253	LUMO	19.5	31.2	1.0	32.8	1.1	
	5	−8.792	HOMO	35.7	11.4	18.0	4.2	19.1	
		−7.662	LUMO	17.7	18.9	4.1	21.0	1.1	27.6
$[(Bz)Cl(PH_3)Ru(=C)_nH_2]^+$	4	−9.369	HOMO	12.3	9.9	16.2	2.7	21.6	
		−7.603	LUMO	6.4	32.0	1.2	33.4		
	5	−9.204	HOMO	12.0	11.5	16.0	4.3	18.7	
		−8.007	LUMO	5.6	19.3	4.6	21.3	1.2	27.9
$[trans\text{-}Cl(PH_3)_2Ru(=C)_nH_2]^+$	4	−8.795	HOMO	30.9	5.7	16.4	1.6	19.4	
		−7.267	LUMO	16.2	33.2	2.7	34.3		
	5	−8.626	HOMO	31.8	6.9	16.2	2.5	15.8	
		−7.736	LUMO	14.9	20.2	4.4	21.8	1.2	28.4
$[(Cp)(PH_3)_2Ru(=C)_nH_2]^+$	4	−8.977	HOMO	32.5	8.5	19.8	2.4	24.4	
		−7.192	LUMO	18.4	30.2	1.6	32.1		
	5	−8.816	HOMO	31.6	8.8	17.1	3.4	18.7	
		−7.635	LUMO	13.4	17.8	5.3	20.1	1.5	26.7

nucleophilic attack. This effect is marked in the series of the cationic Ru(II) complexes, and it is still appreciable going from Cr to W in the $(CO)_5M(=C)_nH_2$ series and is in agreement with the experimentally observed reactivity trends.[1] For instance, in the $(CO)_5Cr=C=C=C(R_1)R_2$ complexes replacing one CO π acceptor by a donor PR_3 ligand strongly reduces the reactivity of the allenylidene chain toward nucleophilic attack.[29] The breakdowns of the contributions from the metal and the carbon atoms along the chain to the HOMO and LUMO are listed in Table 4 and show essentially the same peculiar pattern of $(CO)_5Cr(=C)_nH_2$;[23] the HOMO has contributions mainly from the metal and the carbon atoms in even positions along the chain (C_2, C_4, C_6, ...), while the LUMO has contributions mainly from the carbon atoms in odd positions along the chain (C_1, C_3, C_5, ...), determining the regioselectivity of, respectively, the electrophilic and nucleophilic attack to these atoms in agreement with the experimental reactivity patterns of all known carbon- and heteroatom-substituted metallacumulenes.[1−3,5−9,11,12] It can thus be observed that the localization of the HOMO and LUMO on the even/odd-numbered carbons is essentially unaltered by variations in the electron richness so that no changes in the regioselectivity are foreseen. Therefore, increasing electron richness is expected to give kinetically less reactive complexes without variations in the regioselectivity of nucleophilic and electrophilic attack.

d^8 Complexes: Late Transition Metals. Because $Cl(PPr^i_2)_2Ir(=C)_4Ph_2$[8a] is the only experimentally characterized even-chain metallacumulene, the investigation of this class of group 9 d^8 complexes is an important test for the comparison with the analogous calculated structure. In the present work square-planar complexes of the type *trans*-$M(PH_3)_2Cl(=C)_nH_2$ with $n = 4$, 5 and M = Rh(I), Ir(I) have been studied.

Compared to the group 6 and group 8 d^6 metal fragments considered in the previous paragraph, these fragments have two more electrons in a d_δ orbital, which, although they do not interact with any cumulene orbitals, lead to a more electron-rich character. Many features of their structure and reactivity are therefore similar to those of d^6 metallacumulenes.

The geometries of these complexes, all of C_{2v} symmetry, are reported in Figure 1 and show C−C bond distances close to those observed for d^6 metallacumulenes, with purely cumulenic structures for even-chain complexes and a polyynyl bond alternation for odd-chain complexes. The extent of this alternation is however reduced and is only comparable to that of most electron-rich d^6 metal fragments (e.g., $[Cp(PMe_3)_2Ru]^+$ or $[(CO)_5W]$). This reduction is determined, as before, by the destabilization of the dipolar resonance structures (Scheme 1) with a formal negative charge on the more electron-rich d^8 metal. The M−C distances in all complexes range between 1.84 and 1.86 Å, being slightly longer for C_5 chains. The agreement of the calculated geometries with experimental data for $Cl(PPr^i_2)_2Ir(=C)_4Ph_2$[8a] and $Cl(PPr^i_2)_2Ir(=C)_5Ph_2$[6a] is extremely good, as it can be noted from Table 1. The forseen more allene-like structure of the d^8 metallacumulene complexes is also supported by the low frequencies of the ν(CCC) band in the IR spectra of the experimentally characterized species.[1]

Because the electronic structures of d^8 Rh(I) and Ir(I) metallacumulenes are quite similar, only the diagram for $(PH_3)_2ClIr(=C)_5H_2$ is illustrated in Figure 4, bearing in mind that, as discussed in the previous section, the main difference with the corresponding C_4 and, in general, with even-chain complexes lies in the inversion of their π-conjugated manifolds.

Although an additional filled d_δ orbital characterizes these metal fragments, this orbital does not interact with the cumulene ones and remains as a high lying occupied orbital: it is the HOMO (close to the HOMO−1) for Rh complexes and the HOMO−1 (close to the

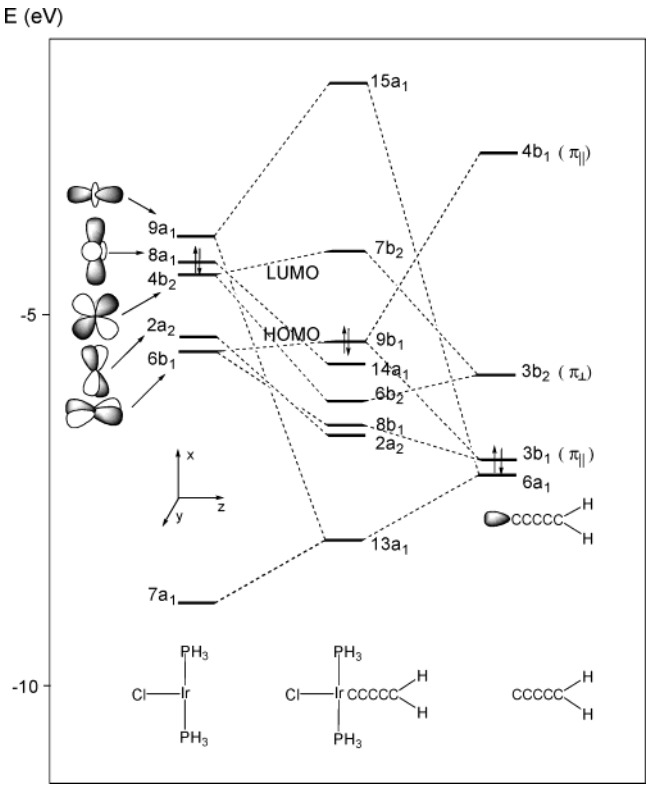

Figure 4. Orbital interaction diagram for the complex *trans*-$Cl(PH_3)_2Ir(=C)_5H_2$.

HOMO) for Ir complexes. Therefore the interaction pattern remains rather similar to that discussed for d^6 complexes with a σ donation from the cumulene lone pair into the d_{z^2} empty orbital of the metal, a π-stabilizing back-donation from one of the filled d_π metal orbitals into the LUMO of cumulene ($\pi_\perp$), and a π partially destabilizing interaction between the remaining d_π metal orbital and the HOMO and LUMO+1 (both $\pi_{||}$) of the cumulene. There are however two main differences between the electronic structures of d^6 and d^8 metal fragments. (i) One is the higher energies of the metal d orbitals, which is especially remarkable for Ir(I), belonging to the third transition series. (ii) The studied d^8 metal fragments result from a square-planar coordination of the metal so that the degeneracy of the d_π orbitals interacting with the cumulene π systems (d_{xz} and d_{yz}) observed in the octahedral and pseudo-octahedral d^6 metal fragments is removed. A splitting of ca. 1 eV is observed with the d_{xz} orbital, lying in the coordination plane, shifted to higher energies.

As a consequence of the energy rise of these metal orbitals, there is a slight decrease of the σ donation and, more importantly, a strong increase of the π back-donation from the in-plane d_{xz} orbital to the cumulene LUMO. On the other hand, the partially destabilizing π interaction between the out-of-plane d_{yz} orbital and the cumulene HOMO remains essentially unchanged.

The effect of the increased π back-donation dominates over the decrease in σ donation, as reflected by the values of the calculated bonding energies (Table 2), which are higher than those for the cationic Ru(II) or the Cr(0), Mo(0), and W(0) carbonyl complexes. In particular, for Ir(I) complexes the metal−cumulene bond is extremely strong, with a dissociation energy more than 100 kJ/mol higher than all the other complexes (see Table 2), thus resulting in thermodynamically very stable compounds. These data can be analyzed using the decomposition scheme of eq 2, whose results are reported in Table 3. It can be noted that, although the small value of E_{prep} contributes to increase the difference between the bonding energies for d^8 and the other complexes, the largest effect is determined by the sharp enhancement in E_{orb}, especially for iridium complexes. In terms of energy decomposition according to the different symmetry contributions, the discussed reduction in σ donation, taking place in the A_1 representation, is negligible, E_{A1} values being very similar to those of the d^6 complexes, if not slightly higher. However what really makes the difference are the values for the stabilizing π back-donation occurring in the B_2 representation, which are much higher than the other cumulenes, while the energies E_{B1}, corresponding to the destabilizing π orbital interaction, remain approximately unvaried.

Like d^6 cumulenes, the reactivity of d^8 complexes is not affected by charge effects (see Table S1) and is again determined by frontier orbital factors. These d^8 complexes present an isolated LUMO and two close highest lying MOs, one of which (the HOMO for Rh, the HOMO−1 for Ir) is essentially a d_δ metal orbital. The breakdown of contributions (see Table 5) from the metal and the cumulene carbon atoms to the LUMO and HOMO (or HOMO−1 for rhodium complexes) shows essentially the same pattern observed for the d^6 octahedral and pseudo-octahedral complexes determining the reactivity of even and odd carbon atoms of the cumulene chains toward, respectively, electrophilic and nucleophilic attack. However, the LUMO of these d^8 complexes is higher in energy, thus leading to a reduced reactivity toward nucleophilic attack, which is responsible for the high reactivity of metallacumulenes and their easy degradation. As a result, one should expect d^8 complexes to be altogether kinetically more stable than the analogous d^6 species. At the same time, also the highest lying MOs of these d^8 complexes are higher in energy, thus allowing an easier electrophilic attack, which is quite unusual for the previously considered d^6 complexes, expecially the Ru(II) cationic ones. Moreover, the presence of the high lying occupied d_δ metal orbital (the HOMO for Rh, the HOMO−1 for Ir) suggests that an orbital-controlled electrophilic attack should occur at the metal center, all the more so, as it is more sterically accessible in the square-planar coordination of these d^8 complexes compared to the octahedral d^6 complexes. Both forecasts are consistent with experimental evidence showing that the synthesized pentatetraenylidene and tetratrienylidene square-planar Ir(I) complexes $(PPh_3)_2ClRh(=C)_nH_2$ and $(PPh_3)_2ClIr(=C)_nH_2$ are quite stable and may undergo electrophilic attack at the metal center (leading to ligand substitution). It is also worth noting that the LUMO of these d^8 complexes shows a significantly larger component on the metal compared to the analogous d^6 species (by about 10%), so that the metal could play a significant role also in the nucleophilic attack.

In summary, d^8 metal fragments are expected to give more stable complexes both from a kinetic and from a thermodynamic point of view, and the metal center may play an important role in their chemistry.

Table 5. Orbital Energies and Breakdowns of the Orbital Contributions from the Metal and Cumulene Carbon Atoms for the Frontier Orbitals of d^8, d^4, and d^2 Complexes

complex	*n*	ϵ	orbital	M	C_1	C_2	C_3	C_4	C_5
$(Cp)_2(PH_3)Ti(=C)_nH_2$	4	−4.421	HOMO	33.0	21.1	2.4	21.2		
		−2.352	LUMO	32.7	11.1	6.4	4.5	13.8	
	5	−4.568	HOMO	28.2	13.7	1.9	16.7	0.0	21.9
		−3.016	LUMO	32.2	7.6	7.8	11.6	2.8	19.0
$[(Cp)(PH_3)_2Mo(=C)_nH_2]^+$	4	−9.318	HOMO-1	36.2	15.0	5.2	18.4		
		−8.397	HOMO	59.60					
		−8.064	LUMO	39.0	1.8	16.8	1.2	20.8	
	5	−9.214	HOMO-1	33.9	9.5	5.8	12.7	2.1	17.7
		−8.441	HOMO	56.11	-				
		−7.873	LUMO	39.1	0.0	18.2	0.0	17.6	
$[trans\text{-}Cl(PH_3)_2Rh(=C)_nH_2]^+$	4	−5.634	HOMO-1	24.8	4.0	13.4	0.0	15.9	
		−5.521	HOMO	64.0					
		−3.980	LUMO	23.4	29.8	2.0	29.1		
	5	−5.613	HOMO-1	26.1	7.3	15.8	2.3	15.7	
		−5.578	HOMO	63.8					
		−4.544	LUMO	22.7	17.0	5.8	17.8	2.0	24.1
$[trans\text{-}Cl(PH_3)_2Ir(=C)_nH_2]^+$	4	−5.507	HOMO	24.3	8.0	19.9	1.7	25.2	
		−3.678	LUMO	25.8	27.2	1.8	26.9		
	5	−5.484	HOMO	24.2	10.2	19.6	3.4	20.7	
		−4.284	LUMO	24.7	15.6	6.3	17.0	2.2	23.3

d^4 and d^2 Complexes: Early Transition Metals. Metallacumulene complexes with d^2 or d^4 metal fragments are quite rare. To the best of our knowledge, a few vinylidenes of the mainly half-sandwich d^4 metal fragment of group 6[12,15b] and one allenylidene derivative of a d^2 metal fragment of group 4, $(Cp)_2(PMe_3)Ti(=C=C=CPh_2)$, have been isolated (see Scheme 1).[14] In the present paper a series of calculation have been carried out on Ti d^2 and Mo d^4 complexes of the type $(Cp)_2PH_3TiC_nH_2$ and $Cp(PH_3)_2MoC_nH_2$ with $n = 4, 5$, to gain some insight into the main structural and electronic properties of these compounds and, eventually, to find an explanation for the marginal role of such complexes in the allenylidene and metallacumulene series.

The geometries of these complexes have been optimized under C_s symmetry and are shown in Figure 1. Both orientations of the cumulene plane with respect to the symmetry plane of the complex were considered, and for either d^4 or d^2 fragments the minimum energy orientation is attained with the C_4H_2 plane lying in the symmetry plane and the C_5H_2 plane lying perpendicular, a reversed situation compared to d^6 and d^8 complexes. This different orientation is a consequence of the different nature of the highest metal d_π orbital, which is of a′ symmetry for d^2 and d^4 fragments and of a″ symmetry for d^6 and d^8 fragments.

A comparison of the calculated structures with experimental geometries is not possible due to the lack of any X-ray data. The C−C bond lengths of the d^2 complexes' cumulene moieties are very similar to those of the corresponding d^6 complexes, with a marked polyyne character in the odd-chain complex and a purely cumulenic character in the even one. For d^4 complexes the situation is reversed: the even-chain metallacumulene shows a pronounced "polyyne-alkynyledene" character, while the odd-chain complex is mainly cumulenic. An explanation for such a behavior can be given by means of a detailed analysis of the orbital interactions (vide infra).

The interaction diagrams for both d^4 and d^2 complexes (see Figures 5 and 6 for the C_5 cumulenes) show that only one of the two d_π orbitals is filled, so that π back-donation occurs only in one plane. Since d^4 and d^2 compounds show different and peculiar interaction

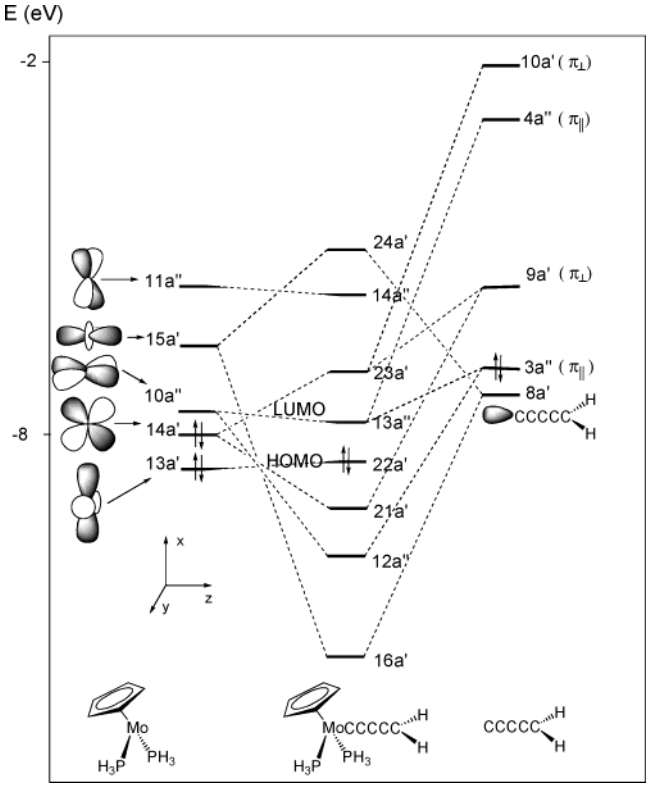

Figure 5. Orbital interaction diagram for the complex $[Cp(PH_3)_2Mo(=C)_5H_2]^+$.

modes with the cumulene moiety orbitals, in the following they will be dealt with separately.

The $[Cp(PH_3)_2Mo]^+$ d^4 fragment has the same frontier orbital pattern of the $[Cp(PH_3)_2Ru]^+$ d^6 fragment: the four valence electrons of the metal are located in $d_{x^2-y^2}$ and d_{xz} orbitals, HOMO−1, and HOMO respectively, while the d_{yz} orbital is now empty and constitutes the LUMO. All orbitals are raised in energy compared to those of the corresponding $[Cp(PH_3)_2Ru]^+$ d^6 complex, as expected for an earlier transition metal. The interaction pattern with the cumulene moiety (see Figure 5 for C_5) shows the same σ donation from the cumulene lone pair to the empty d_{z^2} and π back-donation from the filled d_{xz} to the empty cumulene LUMO observed for the d^6

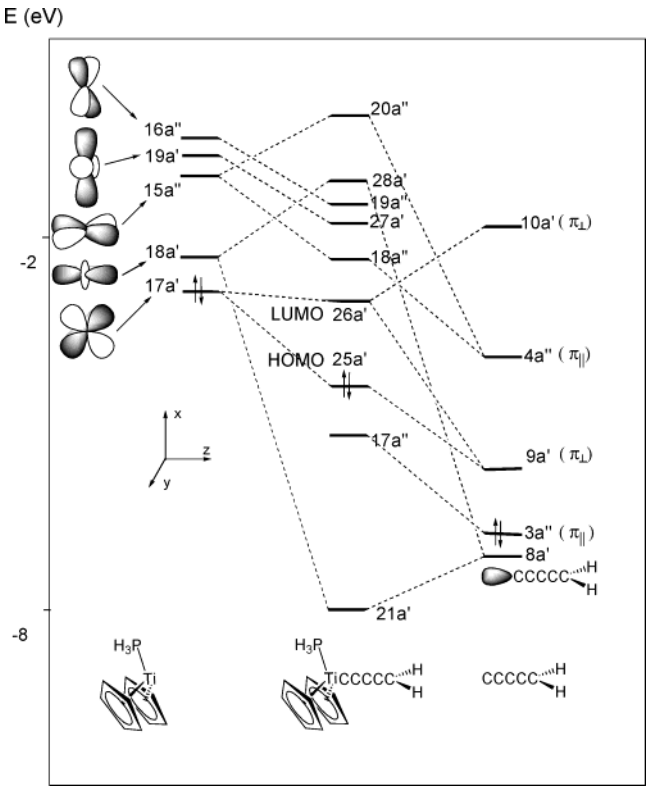

Figure 6. Orbital interaction diagram for the complex $PH_3(Cp)_2Ti(=C)_5H_2$.

and d^8 fragments discussed above. However, since the second d_π (d_{yz}) is empty, the second π interaction in the perpendicular plane between the filled d_{yz} and the filled cumulene HOMO and empty LUMO+1 (corresponding to a destabilizing two-orbital four-electron interactions and to a minor π back-donation interaction, respectively) observed for d^6 and d^8 complexes is now replaced by a stabilizing cumulene to metal π donation.

As a consequence of this different set of interactions, the nature of the metallacumulene frontier orbitals is strongly affected. In particular the correlation between the HOMO of the complex and the HOMO of the cumulene moiety and between the LUMO of the complex and the cumulene LUMO, characteristic of d^6 and d^8 complexes, is now reversed; that is, the highest MO of the complex with cumulene character (the HOMO−1) correlates with the cumulene LUMO, while the LUMO of the complex correlates with the cumulene HOMO. This inversion has important consequences on the geometric structure and reactivity pattern of d^4 complexes. Indeed the different nodal distribution of the HOMO of these d^4 complexes determines the reversed cumulenic geometry of odd-chain and polyyne geometry of even-chain complexes. On the other hand the breakdown of the contributions from the metal and carbon atoms along the chain shows that the HOMO−1 is mainly localized on the odd while the LUMO on the even carbon atoms (see below). Therefore, the localization on even/odd-numbered carbon atoms of the cumulene chain and the regioselectivity toward nucleophilic and electrophilic attacks are inverted with respect to d^6 and d^8 complexes: even carbon atoms are expected to undergo nucleophilic attack and odd carbon atoms electrophilic attack. Since no allenylidene or higher d^4 cumulene complexes have been synthesized so far, a comparison with experimental reactivity pattern is not possible. The low energy of the LUMO and the small HOMO−LUMO gap (ca. 0.5 eV) make this class of metallacumulenes highly reactive, in agreement with the experimental difficulties of synthesizing any allenylidene or higher d^4 cumulene complex.

The absence of any destabilizing two-orbital four-electron interactions and the increased π back-donation (due to the energy increase of the metal d_π orbitals, which come closer to the cumulene LUMO) lead to quite large overall bonding energies, as can be seen in Table 2. As a result, the metal−cumulene bond is strong and d^4 compounds are expected to be thermodynamically quite stable. The energy decomposition by the Ziegler scheme in Table 3 shows indeed that for molybdenum d^4 complexes E_{orb} gives the main contribution to the dissociation energy. The different symmetry of the accepting d_π in d^4 complexes than in the d^6 and d^8 analogues (a′ vs a″) allows a direct comparison only with complexes of C_{2v} symmetry in which the two orthogonal π contributions are separated. The "in-plane" $E_{A'}$ contribution, which takes into account σ donation and π back-donation, is significantly larger when compared with the $E_{A1} + E_{B2}$ contributions (which allow for the same effects) for d^6 metallacumulenes and only slightly lower than in the very stable d^8 complexes, confirming the increased π back-donation in these d^4 complexes. At the same time, the "out-of-plane" $E_{A''}$ is also slightly larger than the corresponding E_{B1} contributions, showing an energy gain on passing from the combined destabilizing two-orbital four-electron and minor π back-donation interactions in d^6 and d^8 complexes to the π donation in d^4 metallacumulenes.

The $[(Cp)_2(PH_3)Ti]$ d^2 fragment, besides having only two electrons in the valence orbitals, differs from d^4— and the analogous d^6—fragments also for the energy level pattern. Indeed, the presence of two Cp ligands induces a destabilization of the $d_{x^2-y^2}$, d_{xy}, and d_{xz}, while the d_{yz} and d_{z^2} are lower in energy and become the HOMO and LUMO of the metal fragment, respectively (Figure 6); moreover, all orbitals are shifted to higher energies, as expected for an earlier transition metal. These two factors, i.e., the different orbital sequence and their increase in energy, affect the bonding interactions with the cumulene moiety. In particular σ donation is expected to be smaller, because of the larger energy gap between the higher energy metal d_{z^2} orbital and the cumulene lone pair, while π back-donation is expected to be larger, because of the high energy of the occupied donating d_{yz} orbital, which become closer to the cumulene LUMO. At variance with the d^4 analogues, these d^2 complexes lack almost any π donation in the plane orthogonal to π back-donation since the d_{xz} orbital, which would have the correct symmetry to interact with the cumulene HOMO, lies too high in energy for such an interaction to take place.

Due to this set of interactions, the HOMO and the LUMO of the d^2 complexes both correlate with the LUMO of the cumulene moiety, a situation different from both d^4 and d^6−d^8 complexes. Indeed, the breakdown of the contributions from the metal and carbon atoms along the chain (see Table 5) shows that both the HOMO and LUMO are mainly localized on the odd carbon atoms. Therefore, the regioselectivity of these

$(Cp)_2PH_3TiC_nH_2$ complexes toward both nucleophilic and electrophilic attacks is directed to odd carbon atoms, the former remaining the same as d^6 and d^8 complexes, the latter being inverted. Unfortunately, no comparison with experimental data is possible since the reactivity of $(Cp)_2PH_3TiC_3Ph_2$, the only synthesized d^2 allenylidene complex,[14] has not been characterized.

As for d^4 complexes, the lack of the destabilizing two-orbital four-electron interaction and the increased π back-donation lead to quite large overall bonding energies (see Table 2) and therefore to thermodynamically quite stable d^2 compounds.

The dissociation energies of d^2 complexes (see Table 2) are quite large and comparable with the highest among those for d^6 complexes but smaller than d^4 complexes, as a consequence of the lack of the π donation. The results of the energy decomposition analysis reported in Table 3 show that the contribution corresponding to σ donation and to π back-donation, occurring in the A′ representation, is quite large, essentially due to the extremely effective π back-donation, and is comparable to that of d^4 complexes and higher than that of most d^6 and d^8 compounds. The value of the $E_{A''}$ contribution is much smaller than for all the other complexes, thus confirming that cumulene to titanium π donation is extremely weak, as discussed above.

The HOMO and the LUMO of d^2 complexes both lie high in energy, so that these complexes are expected to be very reactive with the cumulene chain more exposed to electrophilic rather than nucleophilic attack.

In conclusion d^4 and d^2 electron-poor metal fragments are expected to give thermodynamically stable complexes, because of their peculiar interactions with the cumulene orbitals. However, this does not automatically correspond to a kinetic stability, both d^4 and d^2 complexes being rather reactive under electrophilic and/or nucleophilic attacks, which would explain the experimental difficulty of their synthesis and characterization.

Conclusions

In this paper we performed density functional calculations on a series of metallacumulene complexes $L_mM(=C)_nH_2$ with several ML_m metal fragments to study the electronic structure, the bonding, and the reactivity of these complexes and how they are affected by the metal termini. We considered the metal fragments $[(Cp)_2(PH_3)Ti]$, $[Cp(PH_3)_2Mo]^+$, $[(CO)_5Cr]$, $[(CO)_5Mo]$, $[(CO)_5W]$, $[Cp(dppe)Fe]^+$, [*trans*-$Cl(dppe)_2Ru]^+$, $[Cp(PMe_3)_2Ru]^+$, $[BzCl(PH_3)Ru]^+$, [*trans*-$Cl(PH_3)_2Rh]$, and [*trans*-$Cl(PH_3)_2Ir]$, which are quite common in the chemistry of metal vinylidene, allenylidene, and higher cumulenes and range from a d^2 to a d^8 configuration and from electron-poor to electron-rich character.

The optimized geometries calculated for the considered complexes have been found in good agreement with the available X-ray data and show that the peculiar carbon−carbon bond alternation superimposed to an average cumulenic structure, which is typical of these systems, is only slightly perturbed by the nature of the metal fragment, with the exception of the d^4 $[Cp(PH_3)_2Mo]^+$.

We have calculated bonding energies for all considered systems and discussed their dependence on the nature of the metal termini. We found that an increase of the electron richness within d^6 metal fragments causes a slight decrease of metal−cumulene bond energy. Moreover, bond energies for d^8 and, to a lesser extent, d^4−d^2 complexes are larger than those for the d^6 analogues.

The charge distribution and the localization of the molecular orbitals have been employed to explain the known reactivity patterns of this class of complexes and to forecast their variation with the nature of the metal fragment for both even and odd chains. For d^6 and d^8 complexes, the breakdown of the contributions from the metal and the carbon atoms along the chain to the HOMO and LUMO shows that the HOMO has contributions mainly from the metal and the carbon atoms in even positions along the chain (C_2, C_4, C_6, ...) while the LUMO has contributions mainly from the carbon atoms in odd positions along the chain (C_1, C_3, C_5, ...) determining the regioselectivity of, respectively, the electrophilic and nucleophilic attack to these atoms, in agreement with the experimental reactivity patterns of all known carbon- and heteroatom-substituted metallacumulenes. Therefore, the localization of the HOMO and LUMO on even/odd-numbered carbons is essentially unaltered by variations in the metal electron count from d^6 to d^8 or in the electron richness, so that no changes in the regioselectivity are foreseen. However it is worth noting the presence of a high lying occupied d_δ metal orbital in d^8 complexes, suggesting that an orbital-controlled electrophilic attack should occur at the metal center, all the more so, as it is more sterically accessible in their square-planar coordination. On the other hand, the energy of the LUMOs of the complexes rises with (i) an increase of the electron richness within d^6 series and (ii) an electron count change from d^6 to d^8, thus leading in both cases to a reduced reactivity toward nucleophilic attack. Therefore, increasing electron richness in the d^6 series is expected to give thermodynamically slightly less stable but kinetically less reactive complexes without variations in the regioselectivity of nucleophilic and electrophilic attack. On the other hand, d^8 metal fragments are expected to give more stable complexes both from a kinetic and from a thermodynamic point of view, with the metal center playing an important role in their chemistry.

d^2 and d^4 complexes show peculiar geometric and electronic properties. In particular for d^4 complexes the pattern of C−C bond length is inverted with respect to that typical of d^6 and d^8 metallacumulenes: the even-chain complexes show a pronounced "polyyne-alkynylidene" character, while the odd-chain complexes are mainly cumulenic.

Moreover, for d^4 complexes, the breakdown of the contributions from the metal and carbon atoms along the chain shows that the HOMO is mainly localized on the odd while the LUMO on the even carbon atoms. Therefore, the localization on even/odd-numbered carbon atoms of the cumulene chain and the regioselectivity toward nucleophilic and electrophilic attacks are inverted with respect to d^6 and d^8 complexes: even carbon atoms will undergo nucleophilic attack and odd carbon atoms electrophilic attack. At the same time for d^2 complexes, the HOMO and LUMO are mainly localized

on the odd carbon atoms, so that their regioselectivity toward both nucleophilic and electrophilic attacks is directed to odd carbon atoms, the former remaining the same as d^6 and d^8 complexes, the latter being inverted.

In conclusion d^4 and d^2 electron-poor metal fragments are expected to give thermodynamically stable but kinetically very reactive complexes with a peculiar regioselectivity pattern, which would explain the experimental difficulty of their synthesis and characterization.

Supporting Information Available: Results of Mulliken population analysis: gross atomic charges on the metal and cumulene carbon atoms. This material is available free of charge via the Internet at http://pubs.acs.org.

OM049615L